Published in final edited form as:

Clin Cancer Res. 2015 July 15; 21(14): 3263–3273. doi:10.1158/1078-0432.CCR-14-1200.

Targeting Glutamine Metabolism in Breast Cancer with Aminooxyacetate

Preethi Korangath[1], **Wei Wen Teo**[1], **Helen Sadik**[1], **Liangfeng Han**[1], **Noriko Mori**[2], **Charlotte M. Huijts**[1], **Flonne Wildes**[2], **Santosh Bharti**[2], **Zhe Zhang**[1], **Cesar A. Santa-Maria**[1], **Hualing Tsai**[1], **Chi V. Dang**[3], **Vered Stearns**[1], **Zaver M. Bhujwalla**[2], and **Saraswati Sukumar**[1]

[1]Department of Oncology, Johns Hopkins University School of Medicine, Baltimore, Maryland
[2]Department of Radiology, Johns Hopkins University School of Medicine, Baltimore, Maryland
[3]Department of Medicine, University of Pennsylvania School of Medicine, Philadelphia, Pennsylvania

Abstract

Purpose—Glutamine addiction in c-MYC–overexpressing breast cancer is targeted by the aminotransferase inhibitor, aminooxyacetate (AOA). However, the mechanism of ensuing cell death remains unresolved.

Experimental Design—A correlation between glutamine dependence for growth and c-MYC expression was studied in breast cancer cell lines. The cytotoxic effects of AOA, its correlation with high c-MYC expression, and effects on enzymes in the glutaminolytic pathway were investigated. AOA-induced cell death was assessed by measuring changes in metabolite levels by magnetic resonance spectroscopy (MRS), the effects of amino acid depletion on nucleotide synthesis by cell-cycle and bromodeoxyuridine (BrdUrd) uptake analysis, and activation of the endoplasmic reticulum (ER) stress–mediated pathway. Antitumor effects of AOA with or without common chemotherapies were determined in breast cancer xenografts in immunodeficient mice and in a transgenic MMTV-rTtA-TetO-myc mouse mammary tumor model.

Corresponding Author: Saraswati Sukumar, The Johns Hopkins University School of Medicine, 1650 Orleans Street, CRB1/Room 143, Baltimore, MD 21287. Phone: 410-614-2479; Fax: 410-614-4073; saras@jhmi.edu.

Note: Supplementary data for this article are available at Clinical Cancer Research Online (http://clincancerres.aacrjournals.org/).

Disclosure of Potential Conflicts of Interest

V. Stearns reports receiving commercial research grants from Abbvie, Abraxis, Medimmune, Merck, Novartis, and Pfizer. No potential conflicts of interest were disclosed by the other authors.

Authors' Contributions

Conception and design: P. Korangath, L. Han, C.V. Dang, V. Stearns, S. Sukumar
Development of methodology: P. Korangath, N. Mori, C.V. Dang, S. Sukumar
Acquisition of data (provided animals, acquired and managed patients, provided facilities, etc.): P. Korangath, H. Sadik, N. Mori, F. Wildes, S. Sukumar
Analysis and interpretation of data (e.g., statistical analysis, biostatistics, computational analysis): P. Korangath, W.W. Teo, H. Sadik, N. Mori, S. Bharti, Z. Zhang, H. Tsai, C.V. Dang, V. Stearns, S. Sukumar
Writing, review, and/or revision of the manuscript: P. Korangath, N. Mori, C.M. Huijts, Z. Zhang, C.A. Santa-Maria, H. Tsai, V. Stearns, Z.M. Bhujwalla, S. Sukumar
Administrative, technical, or material support (i.e., reporting or organizing data, constructing databases): P. Korangath, C.M. Huijts, Z.M. Bhujwalla, S. Sukumar
Study supervision: C.V. Dang, S. Sukumar

Results—We established a direct correlation between c-MYC overexpression, suppression of glutaminolysis, and AOA sensitivity in most breast cancer cells. MRS, cell-cycle analysis, and BrdUrd uptake measurements indicated depletion of aspartic acid and alanine leading to cell-cycle arrest at S-phase by AOA. Activation of components of the ER stress–mediated pathway, initiated through GRP78, led to apoptotic cell death. AOA inhibited growth of SUM159, SUM149, and MCF-7 xenografts and c-myc–overexpressing transgenic mouse mammary tumors. In MDA-MB-231, AOA was effective only in combination with chemotherapy.

Conclusions—AOA mediates its cytotoxic effects largely through the stress response pathway. The preclinical data of AOA's effectiveness provide a strong rationale for further clinical development, particularly for c-MYC–overexpressing breast cancers.

Introduction

Metabolic alterations have recently emerged as one of the hallmarks of cancer (1). Cancer cells undergo more rapid replication, and therefore have high biosynthetic and bioenergetic demands. To meet this increasing demand, nutrient uptake and metabolic pathways are altered in cancer cells. Even in the presence of adequate oxygen, cancer cells depend on glycolysis rather than oxidative phosphorylation for energy (2). Recent studies in cancer metabolism have shed light on the role of alternative energy sources, especially glutamine and other amino acids, in cell proliferation and maintenance (3–5), including participation of oncogenes and tumor-suppressor genes in regulating metabolic pathways in cancer cells (6–8).

Recent findings indicate that increased transcriptional activity of *c-MYC* is a characteristic feature of triple-negative breast cancer (TNBC; ref. 9). High c-MYC alters glutamine catabolism, which significantly enhances glutamine uptake, and shifts glutamine metabolic pathways to maintain redox-balance and fuel energy for cell growth (10), rendering it a novel therapeutic target (11). Aminooxyacetate (AOA) is a general inhibitor of pyridoxal phosphate–dependent enzymes, including transaminases, that are involved in amino acid metabolism and has displayed significant antitumor effects as a single agent in preclinical studies (10, 12, 13). In clinical trials of patients with tinnitus (14, 15) and Huntington's disease (16), AOA was well tolerated at approximately 1 to 2 mg/kg/d. At these levels, AOA increased levels of circulating and urinary amino acids (15, 16).

We speculated that AOA inhibits cell growth by depleting the amino acid pool via inhibition of transaminases. Endoplasmic reticulum (ER) stress is then triggered by amino acid deprivation, leading to the activation of unfolded protein response (UPR; ref. 17). A persistent activation of the ER stress pathway will lead to induction of apoptosis (18).

Here, we report the results of a preclinical study of AOA's mode of action and antitumor effects in xenograft models of breast cancer in immunodeficient mice, and in an immune-efficient c-myc transgenic mouse mammary tumor model. The data support a therapeutic role for AOA as a metabolic inhibitor, particularly in c-MYC–overexpressing breast cancer.

Translational Relevance

The transaminase inhibitor, aminooxyacetate (AOA), targets glutaminolytic pathways and displays potent antitumor effects in preclinical models of c-MYC–overexpressing ER-positive and ER-negative breast cancer. Knowledge of the mechanism of action, effectiveness, and tolerability of AOA makes it an excellent candidate for further clinical translation.

Materials and Methods

Cell lines and reagents

Breast cancer cell lines used were those frozen within 6 months of purchase from the ATCC (authenticated using STR profile analysis) and are as follows: MCF-7 (ER/PR^{+ve}/HER2-negative); SKBR3, HCC1954, HCC202 (ER/PR-negative/HER2^{+ve}); BT474 (ER/PR^{+}/HER2^{+ve}); MDA-MB-231, HCC1806, HCC1143 (from ATCC), SUM149 and SUM159 (S. Ethier, MUSC, SC; ER/PR/HER2-negative or triple negative). These two cell lines were not authenticated independently. AOA and biochemicals were purchased from Sigma. Normal human mammary epithelial cells (HMEC) were isolated from reduction mammoplasty samples and grown in MCF10A medium (ATCC). Human breast organoids were prepared by enzymatic digestion of reduction mammoplasty tissue, collected under IRB approved protocols. Mouse tumor cell lines, MTC1 and MTC2 were established from primary mammary tumors in doxycycline-induced MMTV-rTtA-TetO-myc mice, whereas MG1 and MG2 were primary mammary glands from FVB/n litter mates.

MTT assay

Cells were plated in 96-well plates at 1,500 to 5,000 cells per well in 100 μL media. New medium with varying concentration of AOA was added after 12 hours. The assay was performed after 48 hours (19).

Aspartate transaminase assay

Enzyme activity of aspartate transaminase was measured by a colorimetric assay assessing formation of pyruvate from oxaloacetate, a product of GOT1/2 (also called AST1/2) activity, as described previously (20). In brief, cells grown in 6-well plates were collected after 6, 24, or 48 hours of AOA treatment and washed with cold PBS, lysed, and supernatant used for analysis.

Western blot analysis

Antibodies used were as follows: anti–c-MYC (Abcam), GRP78, PERK, IRE1a, CHOP, pAMPK, TAMPK, PARP, c-PARP, c-Cas3 (Cell Signaling Technology), cyclin D1, ATF3 (Invitrogen), β-actin (Sigma). Quantitation was performed using ImageJ software.

Magnetic resonance spectroscopy

SUM159 cells were treated with AOA for 24 hours. Adherent cells were collected by trypsinization and live cells were counted. Water soluble as well as lipid extracts were obtained using the dual-phase extraction method (21).

Cell-cycle analysis and BrdUrd incorporation assay

SUM149 or SUM159 cells were trypsinized after treatment and fixed in 80% ethanol overnight at −20°C. Subsequently, cells were resuspended in a PBS solution containing 20 μg/mL propidium iodide (PI) and 10 μg/mL RNase A and incubated 30 minutes at 37°C (22). For bromodeoxyuridine (BrdUrd) incorporation, cells were treated with BrdUrd (Invitrogen) for 60 minutes at 37°C and washed twice with PBS (23).

Animal experiments

All animal studies were approved by the Institutional Animal Care and Use Committee at Johns Hopkins University. Two million SUM149, SUM159, HCC1954, MDA-MB-231, or 5 million MCF-7 cells resuspended in 50 μL PBS and Matrigel (BD Biosciences; 1:1) were injected s.c. to athymic Balb/c mice (NCI, Frederick). Tumors were measured twice a week.

Transgenic mouse model: Doxycycline-inducible, mammary-specific myc-overexpressing mice (MMTV-rTtA-TetO-myc) were generated as previously described (24).

Statistical analysis

Quantitative data were analyzed using GraphPad Prism (v5.0, GraphPad Software) and SAS software (v9.2, SAS Institute), and expressed as mean ± SD or the percentage of, when appropriate.

Detailed descriptions for each section is provided in Supplementary Methods.

Results

Glutamine dependence of breast cancer cells for growth

The dependence of breast cancer cells on glutamine has not been extensively cataloged. Cells were cultured either in growth medium supplemented with 10% FBS that contained glutamine or was glutamine-free (designated reduced glutamine medium). The growth of breast cancer cell lines MDA-MB-231, SUM149, HCC1806, SUM159, and MCF-7 was dependent on glutamine supplementation. In contrast, BT474, HCC143, HCC1954, HCC202, and SKBR3 were significantly less dependent on glutamine for growth, as assessed by trypan blue staining (Fig. 1A), and also confirmed by colony formation assays (Supplementary Fig. S1A). The number of apoptotic cells increased significantly in glutamine-dependent MDA-MB-231 and SUM149 cell lines grown with reduced glutamine for 6 days, whereas no such change was observed in glutamine-independent BT474 or HCC202 cell lines (Supplementary Fig. S1B).

Differential expression of genes in the glutaminolytic pathway, and sensitivity to AOA

Glutamine provides carbon moieties to the TCA cycle through its entry into mitochondria as alpha-ketoglutarate, either through the activity of glutamate dehydrogenase (GDH) or glutamic oxaloacetate transaminases. Nitrogen from glutamine is essential for biosynthesis of nucleotides and of amino acids glutamate and aspartate, which are the precursors for the synthesis of other nonessential amino acids (Schema in Fig. 1B; ref. 25).

The variable dependence of cancer cells on glutamine could be the consequence of altered expression of genes involved in the glutaminolytic pathway. By RT-qPCR, levels of *GOT1*, *GOT2*, *GPT2*, and *GLS2* (Fig. 1C), but not *GLS1* and *GDH* (Supplementary Fig. S1C) were significantly higher in breast cancer cell lines compared with normal epithelial organoids and cultured HMECs. Interestingly, *GPT2* expression was significantly higher in glutamine-dependent cell lines compared with glutamine-independent cell lines (Fig. 1C). Upon glutamine withdrawal for 24 hours, the expression of *GOT1* increased significantly in MDA-MB-231 and SUM149 cells (Fig. 1D and Supplementary Fig. S1D), but remained unchanged in glutamine-independent BT474 and HCC202, suggesting that GOT1 is one of the key enzymes in glutaminolysis. GPT2 catalyzes a reversible transamination reaction to yield alpha-ketoglutarate and alanine from pyruvate and glutamate. *GPT2* mRNA was higher in all three glutamine-dependent cell lines compared with -independent cell lines (Fig. 1D). These results suggested that elevated GPT2 is also a key enzyme that helps fuel cells to enable survival in a glutamine-poor environment. No specific inhibitors for GOT or GPT2 are currently available. Hence, we tested the effects of pan transaminase inhibition using AOA on survival of 10 ER^+ and ER^- breast cancer cell lines grown in complete medium. Glutamine-dependent cell lines showed greater inhibition of cell growth by AOA compared with cells that were less glutamine dependent (Fig. 2A and Supplementary Fig. S2A). To identify which enzyme activity is targeted by AOA, we used SUM149 cell lines depleted of each enzyme (using siRNA) and tested their sensitivity toward AOA. As shown in Fig. 2B, depletion of GOT1, GOT2, or GPT2 partially reversed AOA-mediated cytotoxic effects. When cells were depleted of GOT1 plus GOT2, or GOT1/2 plus GPT2, cells showed lowered sensitivity to AOA. Interestingly, when cells were depleted of GPT2, both GOT1 and GOT2 levels showed up to 1.6-fold increase (Fig. 2C). These results led to the conclusion that GOT1/2 and GPT2 are partially responsible for AOA-mediated effects, and also suggested compensatory effects following GPT2 depletion, whereby knocking down this enzyme caused the cells to increase the levels of the others. Moreover, cell proliferation was also affected by the knockdown of these genes either alone or in combination in SUM149 cells, which emphasizes the importance of these genes in cell survival (Supplementary Fig. S2B). The enzymatic activity of GOT1/2 tested in three cell lines was also significantly inhibited by AOA in a time-dependent manner (Fig. 2D).

AOA effect on breast cancer cells is c-MYC dependent

Among the earliest molecular aberrations identified in breast cancer, c-MYC amplification and overexpression was reported to occur in 30% to 50% of breast cancers (26). The global effects of c-MYC on metabolism, especially on glutamine metabolism, have been previously studied (27, 28). c-MYC transcriptionally activates the glutamine transporters and glutaminases (29). The role of c-MYC in glutamine addiction has been well studied in

glioblastoma (30) and osteosarcoma (10), but its effect on breast cancer metabolism is not well established. Western blot analysis in a panel of cell lines showed that c-MYC levels are higher than normal in 50% of the tumor cells, and c-MYC levels correlated with glutamine dependence and AOA sensitivity, with a Spearman correlation of r = 0.664; $P = 0.03$ (Fig. 3A). To test the importance of high c-MYC in AOA action, we generated TNBC cells depleted of c-MYC. Transient knockdown of c-MYC in SUM149 and SUM159 (Fig. 3B), and stable depletion in SUM159 cells (Fig. 3B) rendered the cells significantly less sensitive ($P < 0.05$) to AOA-mediated cell death. Compared with control cells, SUM159-sh-cMYC cells were less glutamine dependent for growth (Fig. 3B) and showed a significantly lower expression of glutaminolytic genes, *GOT1* and *GPT2*, but not *GDH* or *GOT2* (Supplementary Fig. S3A). Conversely, overexpression of c-MYC in HCC1954 (low c-MYC) increased AOA sensitivity ($P < 0.05$; Fig. 3C). Collectively, these results demonstrate that AOA sensitivity was significantly greater in cells with high c-MYC expression. This finding was validated using two mouse mammary tumor cell lines, MTC1 and MTC2, established from doxycycline-induced MMTV-rTtA-TetO-myc–driven mammary tumors in FVB/N mice. Both cell lines express high c-myc (maintained in doxycycline-containing medium), were found to be glutamine dependent ($P < 0.001$; Supplementary Fig. S3B and S3C), and were sensitive to growth inhibition by AOA ($P < 0.05$; Fig. 3D). Taking advantage of the inducible *c-myc* present in these cells, we tested the importance of c-myc expression in their response to AOA. A progressive decrease in expression of c-myc in MTC2 cells was achieved by withdrawal of doxycycline from the culture medium. As the c-myc levels decreased over time, the MTC2 cells showed significant loss of sensitivity toward AOA by day 12 (Supplementary Fig. S3D), supporting a significant role of high c-myc expression in the response of the breast cancer tumor cells to AOA.

Magnetic resonance spectroscopic analysis of metabolic changes in AOA-treated cells

Quantitative measures of metabolite alterations in SUM159 cells treated with AOA by magnetic resonance spectroscopy (MRS; metabolite spectra, Supplementary Fig. S4A; ref. 31) showed a significant reduction in aspartate and alanine, and no significant change in glutamate content (Fig. 4A), suggesting AOA-mediated inhibition of aspartate and alanine transaminases. Following AOA treatment, we also observed a reduction in two metabolites associated with neoplastic transformation, total choline (phosphocholine + glycerophosphocholine + freecholine), and phosphocholine (Supplementary Fig. S4B; ref. 32). Ruling out an effect of AOA on the glycolytic pathway, lactate production and glucose consumption measured in the conditioned media collected from AOA-treated SUM159 cells showed no significant changes (Supplementary Fig. S4C). Thus, MRS analysis further confirmed AOA action in depleting alanine and aspartate, and detected a reduction in the established markers of neoplasia, total choline, and phosphocholine.

MRS data suggested that AOA causes depletion of both aspartate and alanine, which are amino acids critical for the growth of many breast cancer cells. If so, exogenous addition of these amino acids should rescue cells from AOA-induced cell death. Cultured MDA-MB-231, SUM149 and SUM159 cells were treated with varying doses of AOA in the presence or absence of alanine or aspartate. Under our experimental conditions, alanine did

not rescue cells from AOA-induced toxicity (Supplementary Fig. S4D and S4E), whereas aspartate rendered cells less sensitive to AOA (Fig. 4B). These data suggested that cell death caused by AOA occurs mainly through aspartate depletion.

AOA causes cell-cycle arrest at S-phase, reversed by aspartate

Aspartate is an amino group donor in nucleotide biosynthesis. Optimal nucleotide levels are necessary for entry into the cell cycle (33). Depletion of aspartate by AOA could, therefore, compromise nucleotide biosynthesis causing cell-cycle arrest at S-phase. Approximately 13% to 15% of exponentially growing SUM159 (Fig. 4C) and SUM149 cells (Supplementary Fig. S5A) are in S-phase. With AOA treatment, an increase in S-phase fraction (32% and 38%, respectively) and a concomitant decrease of cells in G_1 phase was observed. Exogenous aspartate reversed S-phase arrest induced by AOA. The sub-G_1 fraction representing apoptotic cells was also significantly increased in AOA-treated cells (Fig. 4C and Supplementary Fig. S5A). To evaluate the stability of S-phase arrest, SUM159 cells were pulsed with BrdUrd and treated with either fresh medium or with 2 mmol/L AOA. Control cells gradually lost incorporated BrdUrd with each doubling. In AOA-treated cells, however, the number of BrdUrd-positive cells remained unchanged for 72 hours, indicative of a persistent cell-cycle arrest (Fig. 4D). Similar results were obtained with SUM149 cells (Supplementary Fig. S5B). Furthermore, AOA-induced cell-cycle arrest was irreversible, because continued treatment of SUM149 and SUM159 cells for 10 days induced cell death (Supplementary Fig. S5C and S5D). We also evaluated whether exogenous aspartate could substitute glutamine, and reverse cell death. Glutamine-dependent MDA-MB-231, SUM149, SUM159, and HCC1806 cell lines were cultured in normal medium, medium with reduced glutamine, or medium with reduced glutamine supplemented with exogenous aspartate. Exogenous aspartate was able to partially rescue cells from glutamine deprivation-mediated cell death in these cell lines (Supplementary Fig. S5E).

Mechanism of AOA-mediated apoptotic cell death

MRS analysis of metabolites showed that AOA action occurs, in large part, by blocking amino acid metabolism. This, in turn, is known to induce AMPK (activated protein kinase) activation and ER stress in cells. Persistent ER stress leads to cell death through apoptosis (18). To examine these pathways, we treated SUM149 and SUM159 cells with AOA for 24 hours and evaluated mRNA expression and protein levels by RT-qPCR and immunoblotting analysis. AOA treatment significantly increased the mRNA levels of ER stress markers such as *ATF3*, *CHOP*, but not *PERK* (pancreatic ER kinase) or *ATF6* (Fig. 5A). Next, we analyzed whether these alterations are specific to AOA-sensitive cell lines. Western blots analysis of the ER stress markers IRE-1a, GRP78, CHOP, and the apoptosis indicator, cleaved caspase-3, following AOA treatment (2 mmol/L, 72 hours) showed significant increases in levels of stress markers in SUM159 cells compared with control BT474 or HCC202 cell lines (Fig. 5B). GRP78, the ER stress modulator and chaperone for three key sensors, ATF6, PERK, and IRE-1a, showed a 30% decrease in SUM159 cells. A 3-fold increase of IRE-1a (transducer of the ER stress signaling following its dissociation from GRP78), and 12-fold increase in CHOP (the apoptotic inducer in the ER stress pathway) was observed following AOA treatment. A 15-fold increase in cleaved caspase-3 was detected in

SUM159 cells. These data supported specificity of AOA-mediated effects in glutamine-dependent, but not in glutamine-independent cell lines. In addition, Cyclin D1 levels decreased within 24 hours, and AMPK was phosphorylated. Levels of ATF3, acting upstream of CHOP, increased in SUM159 and SUM149 cells. PARP cleavage, another indicator of cell death, was also detected (Supplementary Fig. S6A and S6B). Addition of aspartate in SUM159 cells partially reversed AOA-induced increase in IRE-1a and CHOP, and decrease in levels of GRP78 and cleaved caspase-3 (Fig. 5C).

We also examined the ER stress markers in MDA-MB-231 cells following treatment with AOA combined with the common chemotherapeutic, carboplatin. Carboplatin induced no significant effect on the stress markers, but compared with AOA alone, the combination showed an additive effect on increases in both mRNA and protein levels. The other markers also showed a similar pattern (Supplementary Fig. S6C and S6D). Overall, these data provided strong evidence for induction by AOA of a robust ER stress response through GRP78, IRE-1a, or CHOP, which likely accounts for cell death observed following treatment. A schema outlining the proposed mechanism of action of AOA in c-MYC–overexpressing cancer cells is shown in Fig. 5D.

Antitumor effects of AOA in animal models

Cell culture analysis showed that AOA has growth inhibitory effects, in particular on cells that express high levels of c-MYC protein. We tested the antitumor effects of AOA on xenografts of three high c-MYC–expressing SUM149, SUM159, and MCF-7 breast cancer cell lines, and a low c-MYC–expressing cell line, HCC1954 as a negative control. Treatment with AOA (5 mg/kg) resulted in a significant reduction in tumor growth in SUM149 ($P < 0.01$), SUM159 ($P < 0.001$; Fig. 6A and Supplementary Fig. S7A and S7B), and MCF-7 ($P = 0.001$; Supplementary Fig. S7C) xenografts compared with vehicle control but not in low MYC-expressing, negative control HCC1954 tumors (Fig. 6A). Immunohistochemical analysis of AOA-treated SUM159 and SUM149 tumors showed higher levels of cleaved caspase-3 (Supplementary Fig. S7D). Protein levels of ER stress markers PERK, IRE1, and CHOP were higher in both SUM159 and SUM149 tumors treated with AOA but not in HCC1954 xenografts (Fig. 6B and Supplementary Fig. S7E–S7G). Next, we tested the effect of AOA in combination with carboplatin and paclitaxel, drugs commonly used in the clinic to treat TNBC. No loss of body weight occurred in the immunodeficient recipient mice with AOA treatment (Supplementary Fig. S8A). The combination of AOA with paclitaxel significantly inhibited SUM149 tumor growth compared with paclitaxel alone (Supplementary Fig. S8B), but carboplatin had no addictive effect (Supplementary Fig. S8C). Chemotherapy did not enhance the antitumor effects of AOA in SUM159 tumors (Supplementary Fig. S8D and S8E).

An exception to these observations was noted in MDA-MB-231 cells. Here, despite expression of c-MYC at moderate levels, in culture, cells were very sensitive to AOA. In addition, activation of ER stress and apoptotic pathways occurred in MDA-MB-231 cells treated with AOA alone, with a more pronounced effect when AOA was combined with carboplatin (Supplementary Fig. S6C and S6D). Treated with AOA as a single agent, MDA-MB-231 xenografts did not show any growth inhibition (Fig. 6C). Here, combinations of

AOA with doxorubicin, carboplatin, or paclitaxel resulted in significant ($P < 0.01$) reduction in size of tumors. Western blot analysis of a representative set of tumors showed that treatment with carboplatin or doxorubicin alone resulted in a nearly 2-fold increase in the level of c-MYC protein compared with either vehicle control or AOA treatment (Supplementary Fig. S8F). These data raised the possibility that susceptibility to AOA correlates not only with constitutive, but also with chemotherapy-induced overexpression of c-MYC protein. Also, effectiveness of treatment with AOA as a single agent or in combination with chemotherapy may be predicted by c-MYC levels in the pretreatment tumor biopsy. In addition, posttreatment upregulation of c-MYC could contribute to greater sensitivity of AOA.

To further substantiate our findings, we used the doxycycline-inducible MMTV-driven myc-overexpressing transgenic mouse model. Upon doxycycline induction, the bitransgenic mice develop mammary tumors with a latency of around 22 weeks (24). When tumors reached a size of 150 to 200 mm^3, mice were treated with AOA at 0.5 mg/kg body weight per 3 days a week for 4 weeks ($n = 5–10$/group). There was a significant reduction in tumor growth in mice treated with AOA (Fig. 6D). In contrast with Balb/c nu/nu mice, doses of AOA above 0.5 mg/kg (doses tested, 0.5, 1, 2.5, and 5 mg/kg) caused loss of body weight and death in this strain of mouse.

Discussion

The role of glutamine metabolism on proliferation has not yet been studied extensively in breast cancer, particularly in TNBC. In this study, we have provided evidence that breast cancer cell lines that express high levels of c-MYC are dependent on glutamine for their survival and growth. Suppression of glutaminolysis in these cell lines using a transaminase inhibitor, AOA, resulted in cell death, largely through activation of the ER stress pathway. These findings led us to further develop AOA in breast cancer as a therapeutic target.

Inhibition of glutamine metabolism is an active area of research. As a result several agents targeting glutamine metabolism are under development (34). In 2008, researchers reported that treatment of a single cell line, MDA-MB-231 with AOA resulted in a decrease in alanine and flux of ^{13}C-glucose–derived carbons into glutamate and uridine, and a reduction in oxygen consumption rate, cellular ATP level and NAD^+/NADH ratio (13). In this study, we have reported an in depth characterization of AOA-mediated cell death pathways in breast cancer cells. The expression level and activity of many enzymes essential for glutamine metabolism, including GOT1, GOT2, GPT2, and GLS2, were highly elevated in breast cancer cell lines compared with normal breast cells. This reliance on alternative sources of energy, in all likelihood, forms the basis for the addiction of the breast cancer cells to glutamine. A second factor contributing to glutamine addiction could be high levels of c-MYC expression in cells (30). If so, it stands to reason that c-MYC–overexpressing cells will be particularly sensitive to transaminase inhibitors such as AOA. In fact, we found a significant correlation between c-MYC level and drug sensitivity (Fig. 3A–C). Our data are consistent with published findings where ATF4 andits downstream regulators were found to be critical mediators of apoptosis consequent to glutamine withdrawal in c-MYC–overexpressing neuroblastoma (12). In TNBC cells, AOA treatment lowered levels of the

chaperone protein, GRP78, and activated many ER stress pathway genes, including ATF3, downstream of ATF4. Stresses in the tumor microenvironment such as low oxygen, low glucose, and decreased amino acid availability activate UPR, a cellular homeostatic program triggered by an excess of misfolded or unfolded proteins in the ER lumen (18). During prolonged stress, UPR initiates a program leading to apoptosis. The three proximal effectors of the UPR are PERK, activating transcription factor 6 (ATF6), and inositol-requiring transmembrane kinase/endonuclease 1 (IRE1). Autophosphorylation of PERK permits the translation of specific cap-independent ER stress response genes, such as ATF4. The proapoptotic protein CHOP (CCAAT/-enhancer–binding protein homologous protein), is upregulated downstream of ATF4, causes downregulation of the antiapoptotic mitochondrial protein Bcl-2, promoting apoptosis. Second, ATF6 is activated by proteolytic cleavage following translocation to the Golgi (35). IRE1a activates a JNK signaling pathway, at which point human pro–caspase-4 is believed to cause apoptosis by activating downstream caspases (18). The mammalian adenosine monophosphate–activated protein kinase (AMPK) is a serine–threonine kinase protein complex that is a central regulator of cellular energy homeostasis; the mechanisms by which AMPK mediates cellular responses to metabolic stress remain unclear (36). We have shown here that ER stress may constitute a major pathway in cell growth inhibition caused by AOA treatment.

We also propose a novel mechanism of cell growth inhibition by AOA. It is well known that glutamine and aspartate provide the amine groups that are critical for nucleoside synthesis. The reduction in the nucleoside pool in the cell may cause cell-cycle arrest in S-phase as shown by our cell-cycle analysis and BrdUrd incorporation assay (37). In our study, aspartate alone effectively decreased AOA sensitivity to breast cancer cells and reversed S-phase arrest, which could be attributed possibly to the rescue of nucleotide synthesis by aspartate. Another interesting finding was the effect of AOA on choline metabolism as observed in the MRS studies. Elevated levels of phosphocholine and total choline have been reported in malignant breast tumors (32, 38, 39). The role of AOA in decreasing total choline and phosphocholine remains to be investigated.

Although MDA-MB-231 cells were sensitive to AOA *in vitro*, contrary to the published report (13), which observed the AOA-treated mice (10 mg/kg body weight) for only 2 weeks, we did not observe tumor growth inhibition at 5 mg/kg body weight of AOA. In our hands, larger doses were associated with loss of weight and signs of toxicity after a week, especially severe when combined with chemotherapeutic agents. Whether MDA-MB-231 cells overcome AOA-induced ER stress–mediated cell death *in vivo* through cross-talk with the microenvironment needs further investigation.

AOA had a potent growth inhibitory effect on MMTV-rTtA-TetO-myc transgenic mouse mammary tumors. By taking advantage of the doxycycline inducibility of the gene in this system, we have demonstrated that myc depletion reverses AOA susceptibility of the tumor cells. These findings, in addition, provide a strong rationale for exploring the utility of this small molecule in c-MYC–overexpressing breast tumors. AOA may be an appealing therapeutic agent based on its high tolerability and strong anti-tumor effects, providing a strong rationale for further drug development.

In summary, we have shown that breast cancer cells, particularly TNBCs, are dependent on glutamine for growth and this dependence can be effectively targeted by AOA. The ER stress pathway induced by AOA leads to cell growth inhibition and apoptosis. AOA, while cytotoxic to tumor cells, has shown acceptable toxicity profiles in small clinical trials, which may allow for rapid drug development. Furthermore, because preclinical data suggest a role for glutamine metabolism in multiple other cancer types, specifically sarcomas, brain tumors, and other c-MYC–driven cancers, AOA may have a wider therapeutic application.

Supplementary Material

Refer to Web version on PubMed Central for supplementary material.

Acknowledgments

The authors thank Dr. Lewis Chodosh, University of Pennsylvania for generously providing MMTV-rTtA-tetO-myc transgenic mice and Dr. A. Goga for providing the c-MYC overexpression vector. The authors thank Dileep Unnikrishnan and Sidra Hafeez for laboratory assistance.

Grant Support

This research was supported by Department of Defense Center of Excellence grant W81XWH-04-1-0595 (to S. Sukumar); Susan Komen Foundation for the Cure Postdoctoral grant (PDF12231403; to P. Korangath); the Cindy Rosencrans Fund for Triple-Negative Breast Cancer Research (to V. Stearns), and the SKCCC Core grant P30 CA006973 (to S. Sukumar).

References

1. Hanahan D, Weinberg RA. Hallmarks of cancer: the next generation. Cell. 2011; 144:646–74. [PubMed: 21376230]
2. Warburg O. On the origin of cancer cells. Science. 1956; 123:309–14. [PubMed: 13298683]
3. DeBerardinis RJ, Lum JJ, Hatzivassiliou G, Thompson CB. The biology of cancer: metabolic reprogramming fuels cell growth and proliferation. Cell Metab. 2008; 7:11–20. [PubMed: 18177721]
4. Sheen JH, Zoncu R, Kim D, Sabatini DM. Defective regulation of autophagy upon leucine deprivation reveals a targetable liability of human melanoma cells *in vitro* and *in vivo*. Cancer Cell. 2011; 19:613–28. [PubMed: 21575862]
5. Possemato R, Marks KM, Shaul YD, Pacold ME, Kim D, Birsoy K, et al. Functional genomics reveal that the serine synthesis pathway is essential in breast cancer. Nature. 2011; 476:346–50. [PubMed: 21760589]
6. Gao P, Tchernyshyov I, Chang TC, Lee YS, Kita K, Ochi T, et al. c-Myc suppression of miR-23a/b enhances mitochondrial glutaminase expression and glutamine metabolism. Nature. 2009; 458:762–5. [PubMed: 19219026]
7. Maddocks OD, Berkers CR, Mason SM, Zheng L, Blyth K, Gottlieb E, et al. Serine starvation induces stress and p53-dependent metabolic remodelling in cancer cells. Nature. 2013; 493:542–6. [PubMed: 23242140]
8. Mauro C, Leow SC, Anso E, Rocha S, Thotakura AK, Tornatore L, et al. NF-kappaB controls energy homeostasis and metabolic adaptation by upregulating mitochondrial respiration. Nat Cell Biol. 2011; 13:1272–9. [PubMed: 21968997]
9. Alles MC, Gardiner-Garden M, Nott DJ, Wang Y, Foekens JA, Sutherland RL, et al. Meta-analysis and gene set enrichment relative to er status reveal elevated activity of MYC and E2F in the “basal” breast cancer subgroup. PLoS ONE. 2009; 4:e4710. [PubMed: 19270750]
10. Anso E, Mullen AR, Felsher DW, Mates JM, Deberardinis RJ, Chandel NS. Metabolic changes in cancer cells upon suppression of MYC. Cancer Metab. 2013; 1:7. [PubMed: 24280108]

11. Dang CV. Therapeutic targeting of Myc-reprogrammed cancer cell metabolism. Cold Spring Harb Symp Quant Biol. 2011; 76:369–74. [PubMed: 21960526]
12. Qing G, Li B, Vu A, Skuli N, Walton ZE, Liu X, et al. ATF4 regulates MYC-mediated neuroblastoma cell death upon glutamine deprivation. Cancer Cell. 2012; 22:631–44. [PubMed: 23153536]
13. Thornburg JM, Nelson KK, Clem BF, Lane AN, Arumugam S, Simmons A, et al. Targeting aspartate aminotransferase in breast cancer. Breast Cancer Res. 2008; 10:R84. [PubMed: 18922152]
14. Reed HT, Meltzer J, Crews P, Norris CH, Quine DB, Guth PS. Amino-oxyacetic acid as a palliative in tinnitus. Arch Otolaryngol. 1985; 111:803–5. [PubMed: 2415097]
15. Guth PS, Risey J, Briner W, Blair P, Reed HT, Bryant G, et al. Evaluation of amino-oxyacetic acid as a palliative in tinnitus. Ann Otol Rhinol Laryngol. 1990; 99:74–9. [PubMed: 1688487]
16. Perry TL, Wright JM, Hansen S, Allan BM, Baird PA, MacLeod PM. Failure of aminooxyacetic acid therapy in Huntington disease. Neurology. 1980; 30:772–5. [PubMed: 6446691]
17. Hetz C, Chevet E, Harding HP. Targeting the unfolded protein response in disease. Nat Rev Drug Discov. 2013; 12:703–19. [PubMed: 23989796]
18. Szegezdi E, Logue SE, Gorman AM, Samali A. Mediators of endoplasmic reticulum stress-induced apoptosis. EMBO Rep. 2006; 7:880–5. [PubMed: 16953201]
19. van de Loosdrecht AA, Beelen RH, Ossenkoppele GJ, Broekhoven MG, Langenhuijsen MM. A tetrazolium-based colorimetric MTT assay to quantitate human monocyte mediated cytotoxicity against leukemic cells from cell lines and patients with acute myeloid leukemia. J Immunol Methods. 1994; 174:311–20. [PubMed: 8083535]
20. Bergmeyer, HUBE. Colorimetric assay of Reitman and Frankel. New York: Academic Press; 1974.
21. Glunde K, Raman V, Mori N, Bhujwalla ZM. RNA interference-mediated choline kinase suppression in breast cancer cells induces differentiation and reduces proliferation. Cancer Res. 2005; 65:11034–43. [PubMed: 16322253]
22. van Engeland M, Ramaekers FC, Schutte B, Reutelingsperger CP. A novel assay to measure loss of plasma membrane asymmetry during apoptosis of adherent cells in culture. Cytometry. 1996; 24:131–9. [PubMed: 8725662]
23. Campana D, Coustan-Smith E, Janossy G. Double and triple staining methods for studying the proliferative activity of human B and T lymphoid cells. J Immunol Methods. 1988; 107:79–88. [PubMed: 3257781]
24. D'Cruz CM, Gunther EJ, Boxer RB, Hartman JL, Sintasath L, Moody SE, et al. c-MYC induces mammary tumorigenesis by means of a preferred pathway involving spontaneous Kras2 mutations. Nat Med. 2001; 7:235–9. [PubMed: 11175856]
25. Vander Heiden MG, Cantley LC, Thompson CB. Understanding the War-burg effect: the metabolic requirements of cell proliferation. Science. 2009; 324:1029–33. [PubMed: 19460998]
26. Horiuchi D, Kusdra L, Huskey NE, Chandriani S, Lenburg ME, Gonzalez-Angulo AM, et al. MYC pathway activation in triple-negative breast cancer is synthetic lethal with CDK inhibition. J Exp Med. 2012; 209:679–96. [PubMed: 22430491]
27. Liu W, Le A, Hancock C, Lane AN, Dang CV, Fan TW, et al. Reprogramming of proline and glutamine metabolism contributes to the proliferative and metabolic responses regulated by oncogenic transcription factor c-MYC. Proc Natl Acad Sci U S A. 2012; 109:8983–8. [PubMed: 22615405]
28. Dang CV. Rethinking the Warburg effect with Myc micromanaging glutamine metabolism. Cancer Res. 2010; 70:859–62. [PubMed: 20086171]
29. Li F, Wang Y, Zeller KI, Potter JJ, Wonsey DR, O'Donnell KA, et al. Myc stimulates nuclearly encoded mitochondrial genes and mitochondrial biogenesis. Mol Cell Biol. 2005; 25:6225–34. [PubMed: 15988031]
30. Wise DR, DeBerardinis RJ, Mancuso A, Sayed N, Zhang XY, Pfeiffer HK, et al. Myc regulates a transcriptional program that stimulates mitochondrial glutaminolysis and leads to glutamine addiction. Proc Natl Acad Sci U S A. 2008; 105:18782–7. [PubMed: 19033189]
31. Kinoshita Y, Yokota A. Absolute concentrations of metabolites in human brain tumors using *in vitro* proton magnetic resonance spectroscopy. NMR Biomed. 1997; 10:2–12. [PubMed: 9251109]

32. Glunde K, Jie C, Bhujwalla ZM. Molecular causes of the aberrant choline phospholipid metabolism in breast cancer. Cancer Res. 2004; 64:4270–6. [PubMed: 15205341]

33. Ewald B, Sampath D, Plunkett W. Nucleoside analogs: molecular mechanisms signaling cell death. Oncogene. 2008; 27:6522–37. [PubMed: 18955977]

34. Bobrovnikova-Marjon E, Hurov JB. Targeting metabolic changes in cancer: novel therapeutic approaches. Annu Rev Med. 2014; 65:157–70. [PubMed: 24422570]

35. Crespo I, San-Miguel B, Prause C, Marroni N, Cuevas MJ, Gonzalez-Gallego J, et al. Glutamine treatment attenuates endoplasmic reticulum stress and apoptosis in TNBS-induced colitis. PLoS ONE. 2012; 7:e50407. [PubMed: 23209735]

36. Wirth M, Joachim J, Tooze SA. Autophagosome formation—the role of ULK1 and Beclin1-PI3KC3 complexes in setting the stage. Semin Cancer Biol. 2013; 23:301–9. [PubMed: 23727157]

37. Jordheim LP, Durantel D, Zoulim F, Dumontet C. Advances in the development of nucleoside and nucleotide analogues for cancer and viral diseases. Nat Rev Drug Discov. 2013; 12:447–64. [PubMed: 23722347]

38. Jacobs MA, Barker PB, Bottomley PA, Bhujwalla Z, Bluemke DA. Proton magnetic resonance spectroscopic imaging of human breast cancer: a preliminary study. J Magn Reson Imaging. 2004; 19:68–75. [PubMed: 14696222]

39. Baik HM, Su MY, Yu H, Mehta R, Nalcioglu O. Quantification of choline-containing compounds in malignant breast tumors by 1H MR spectroscopy using water as an internal reference at 1. 5 T. MAGMA. 2006; 19:96–104. [PubMed: 16779565]

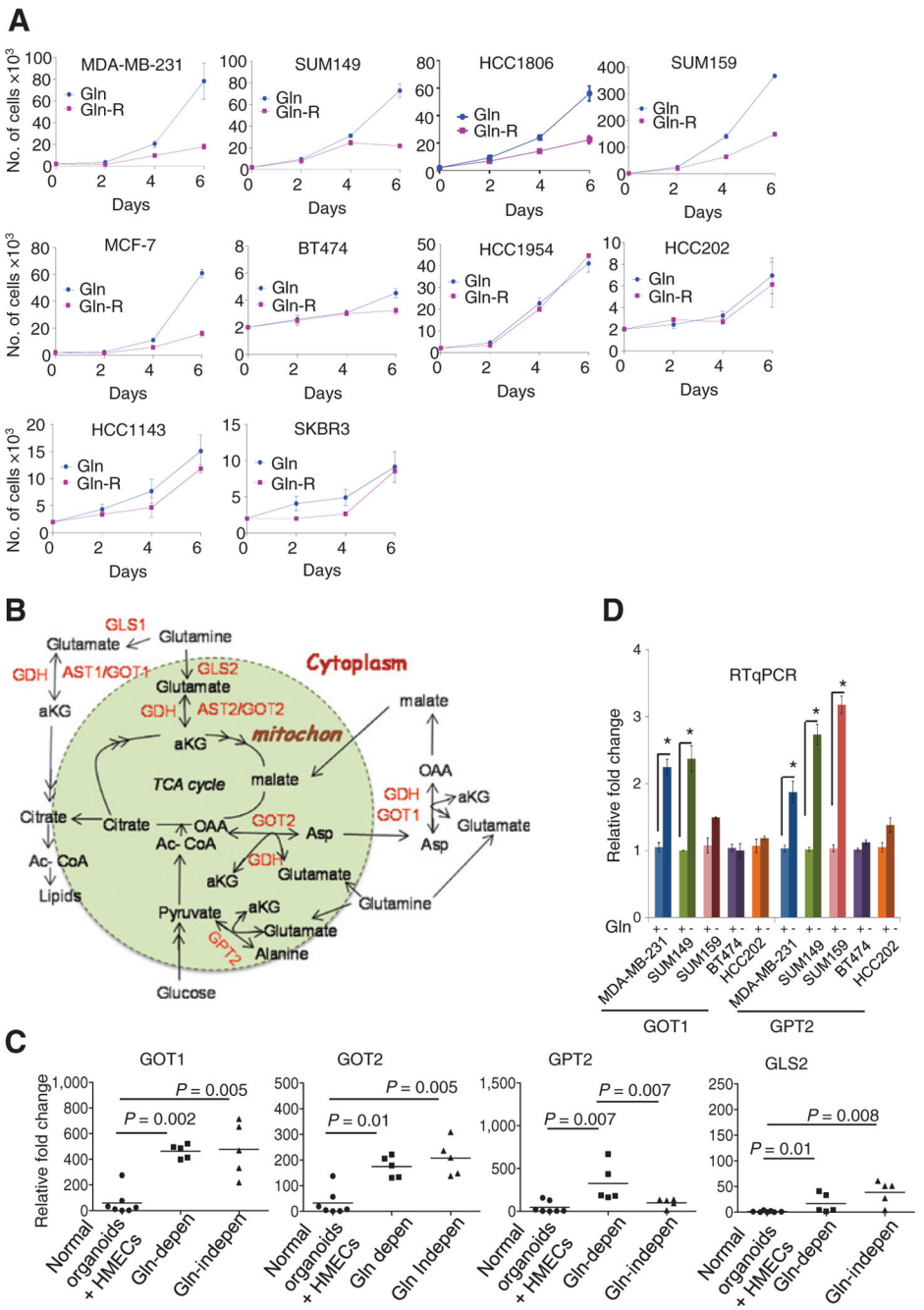

Figure 1.

Glutamine dependency of breast cancer cell lines. A, breast cell lines were grown in media with complete or reduced glutamine (Gln and Gln-R). The average number of live cells per well (3-wells/time point; two replicates), on indicated days is shown. B, schematic representation of transaminases and other genes involved in glutaminolysis. C, differential mRNA expression of *GOT1*, *GOT2*, *GLS2*, and *GPT2* in breast cancer cell lines compared with normal mammary organoids and HMECs (duplicates in each assay; three replicates). The Mann–Whitney test, *, $P < 0.05$. D, RT-qPCR of genes in the glutaminolytic pathway

following growth in medium with complete (Gln^+) or reduced glutamine (Gln^-) for 24 hours (duplicates in each assay; three replicates); the Mann–Whitney test; *, $P < 0.05$.

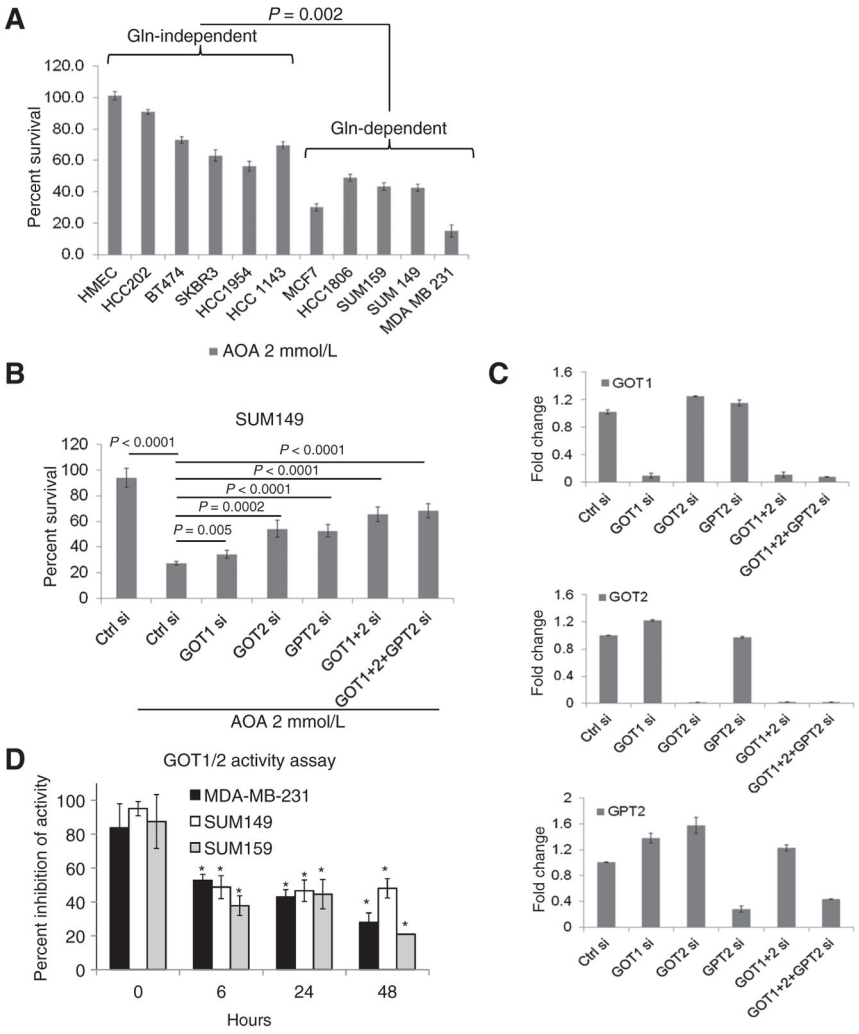

Figure 2.

Sensitivity of breast cancer cells to AOA and its reversal in cells depleted of GOT1/2 and GPT2. A, MTT assay of breast cancer cell lines and normal HMECs after treatment with 2 mmol/L AOA for 48 hours. B, reversal of cytotoxic effects of AOA in SUM149 cells depleted of GOT1, GOT2, and GPT2. C, RT-qPCR of *GOT1*, *GOT2*, and *GPT2* mRNA in SUM149 cells depleted of the indicated genes. D, enzymatic activity of GOT1 and GOT2 after AOA treatment (2 mmol/L) shows significant inhibition following 6 hours of exposure. Each experiment was repeated three times. All statistical analysis by Student *t* test; two-tailed; *, $P < 0.05$.

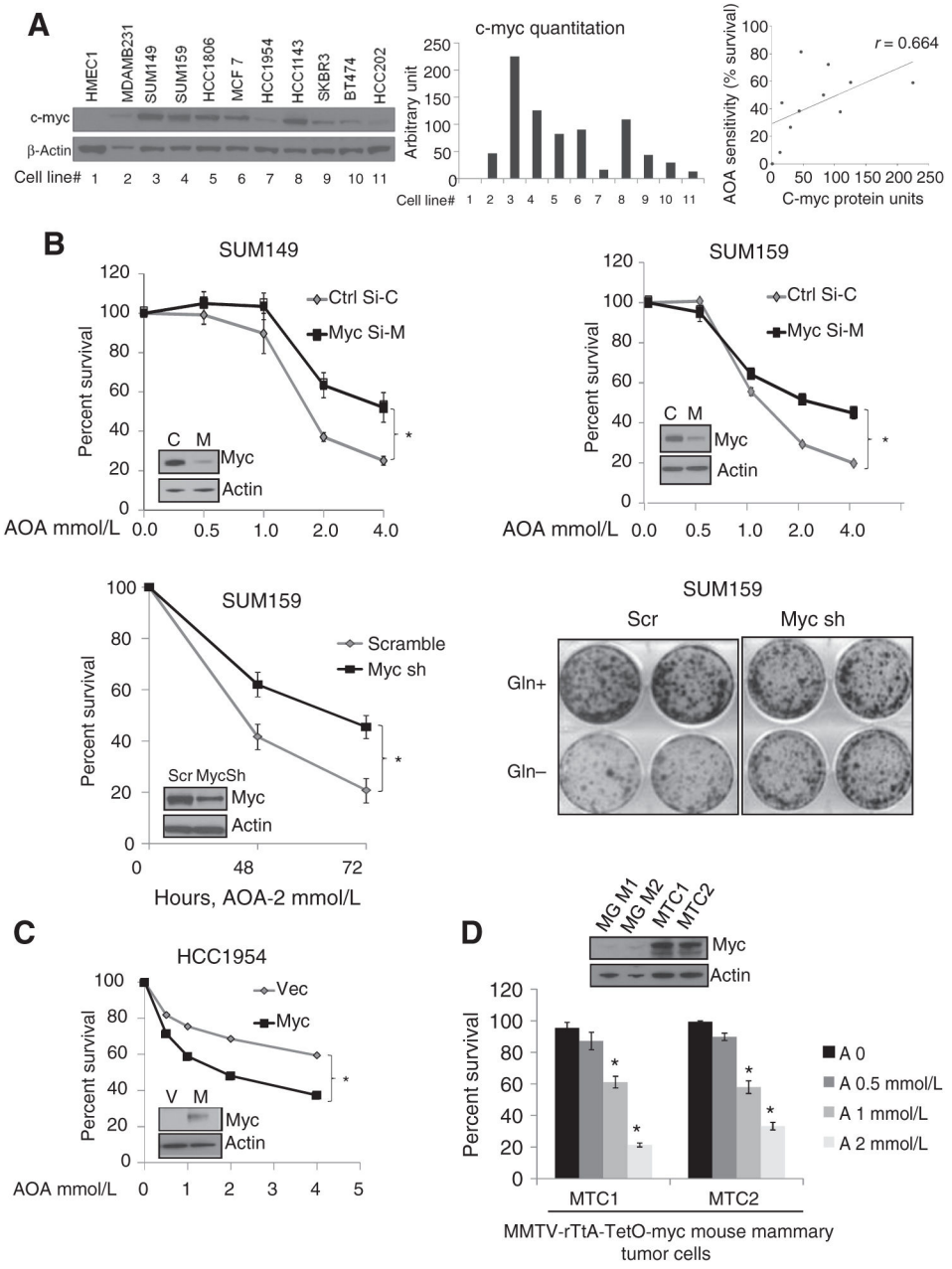

Figure 3.

AOA sensitivity is c-MYC dependent. A, Western blot analysis of c-MYC protein in breast cancer cells; densitometry evaluation normalized with loading control β-actin; and correlation between c-MYC protein level and sensitivity to AOA. The percentage of cells surviving after 48 hours of treatment with 2 mmol/L AOA (from Fig. 2A) was plotted against quantity of c-MYC protein in the same cell line. Spearman correlation $r = 0.664$; *, $P < 0.05$. B, siRNA-mediated depletion of c-MYC in SUM149 and SUM159 cells. MTT assay of cells treated with AOA for 48 hours. Sensitivity of SUM159 cells stably expressing c-MYC shRNA compared with scramble (Scr) shRNA-expressing cells (left) to AOA; colony formation assay showing that MYC-depleted SUM159 cells are not dependent on glutamine

for growth (right). C, MTT assay to test the effect of AOA in HCC1954 breast cancer cells overexpressing exogenous c-MYC. D, MTT assay to test the effect of AOA in two mouse mammary tumor cell lines. Western blot analysis shows c-myc overexpression in two tumor cell lines, MTC1 and MTC2, compared with uninduced FVB/N mouse mammary glands, MG1 and MG2. Values are represented as mean ± SD of three independent experiments, with 4-wells tested for each condition for B to D. All the data were analyzed by the Student *t* test, two-tailed; *, $P < 0.05$.

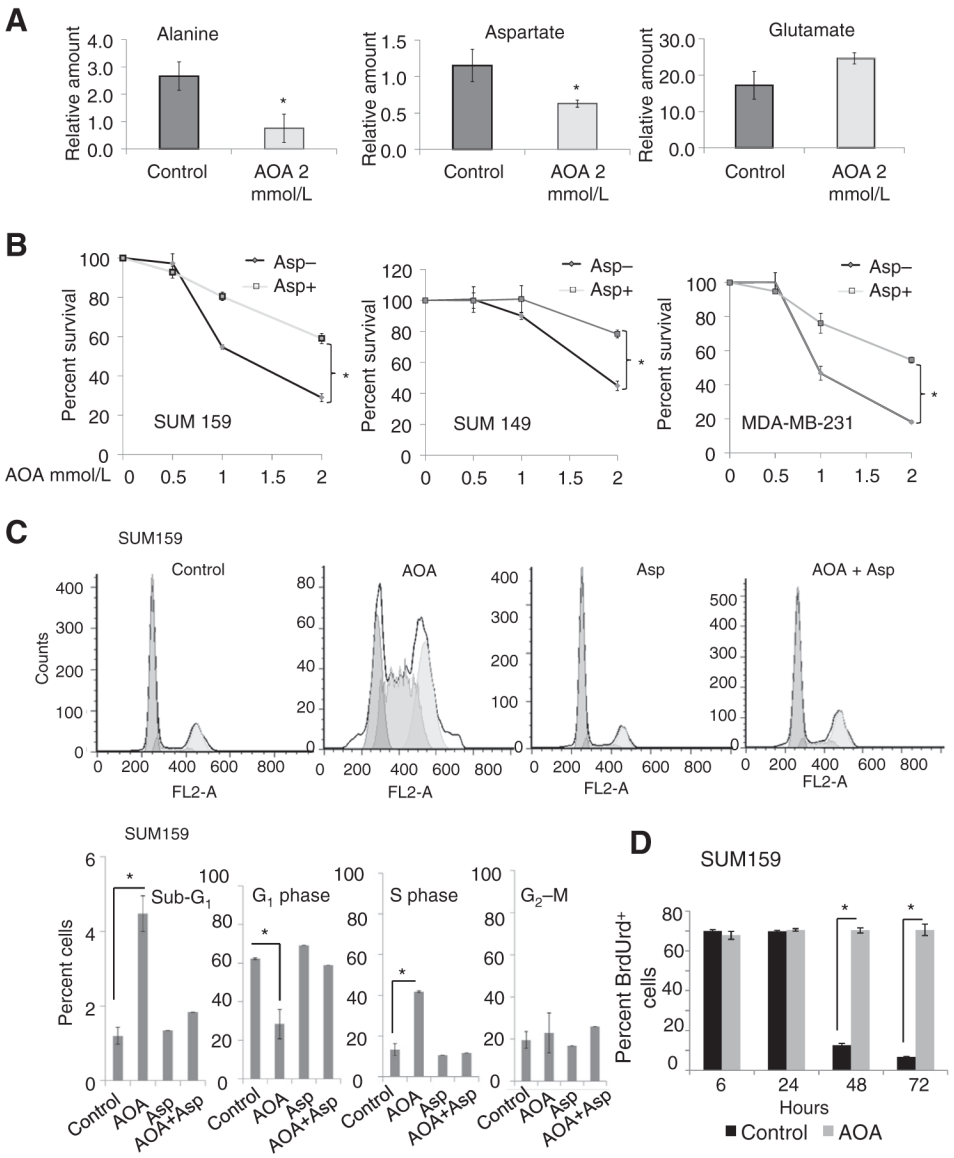

Figure 4.

A, MRS analysis of SUM159 cells treated with AOA showing significant decrease in alanine and aspartate, but not glutamate (*, $P < 0.05$). B, MTT assay showing the percentage of viable cells in culture in the presence of 10 mmol/L aspartate with varying amounts of AOA for 48 hours (*, $P < 0.01$). C, AOA induces S-phase arrest, reversed by adding aspartate. Flow-cytometry analysis of cell cycle in SUM159 cells exposed to vehicle, AOA, aspartate, or AOA + aspartate for 72 hours using PI showing increase in sub-G_1 content and S-phase arrest in AOA-treated cells; this effect was reversed by cotreatment with aspartate. D, stability of S-phase arrest by BrdUrd incorporation and retention. Cells were stained for BrdUrd and PI, and analyzed by flow cytometry showed significant increase of BrdUrd positive cells after 48 and 72 hours of AOA (2 mmol/L) treatment. Values are represented as mean ± SD of three independent experiments for A to D. All the data were analyzed by the Student *t* test, two-tailed.

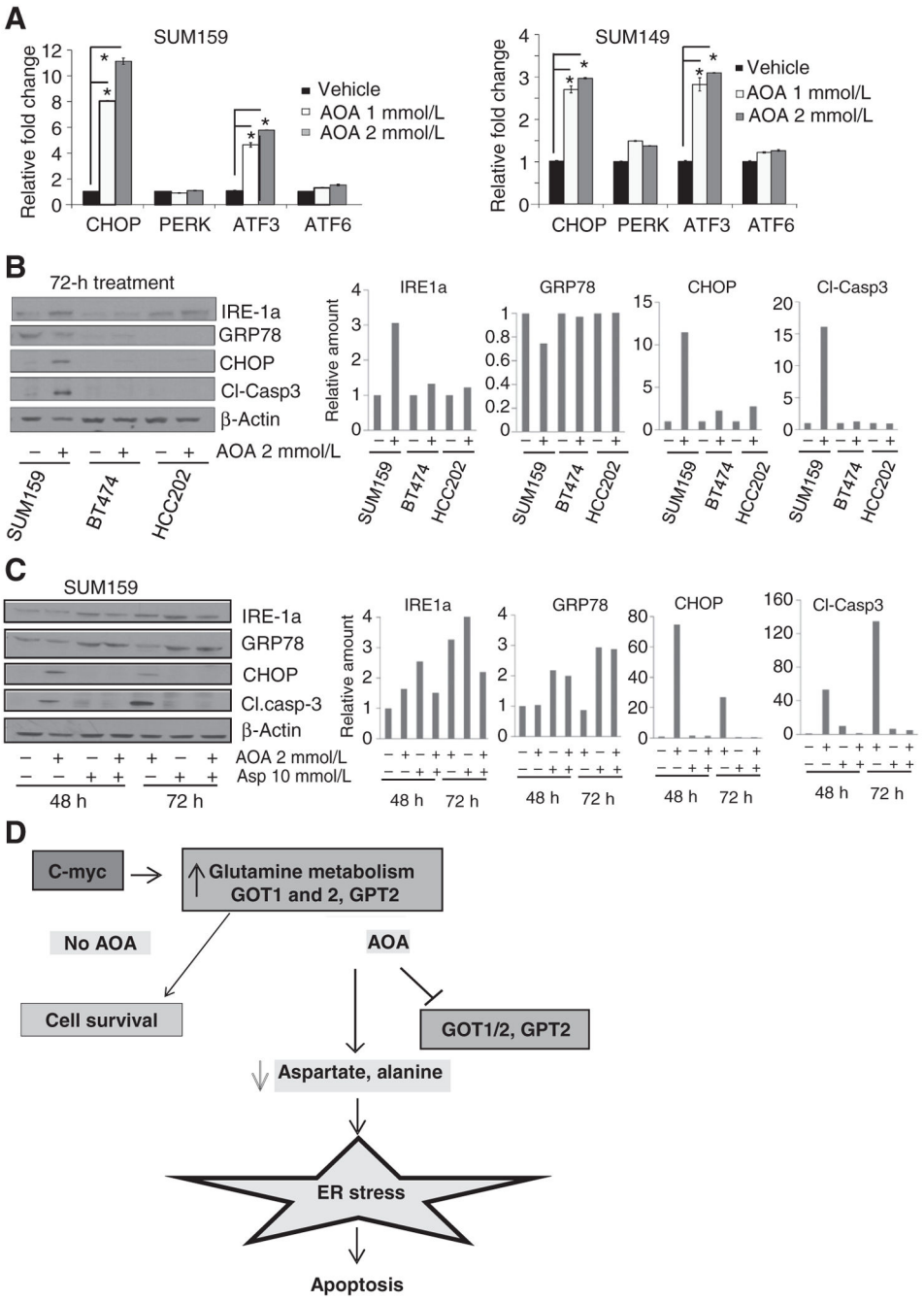

Figure 5.

Molecular mechanism of AOA-induced growth inhibition and death. A, RT-qPCR analysis of SUM159 and SUM149 cells showing induction of ER stress markers after 24 hours exposure to 2 mmol/L AOA (duplicates in each assay; three replicate assays). The Student *t* test, two-tailed *, $P \leq 0.05$. B, Western blot analysis for stress markers and apoptotic marker caspase-3 comparing AOA-sensitive SUM159 with AOA-insensitive BT474 and HCC202 cell lines after 72 hours exposure to 2 mmol/L AOA. C, induction of ER stress markers and caspase-3 is reversed by addition of aspartate to SUM159 and SUM149 cells following 48

or 72 hours of treatment with AOA; bar graph, quantitation. D, schema of proposed mechanism of action of AOA in breast cancer cells.

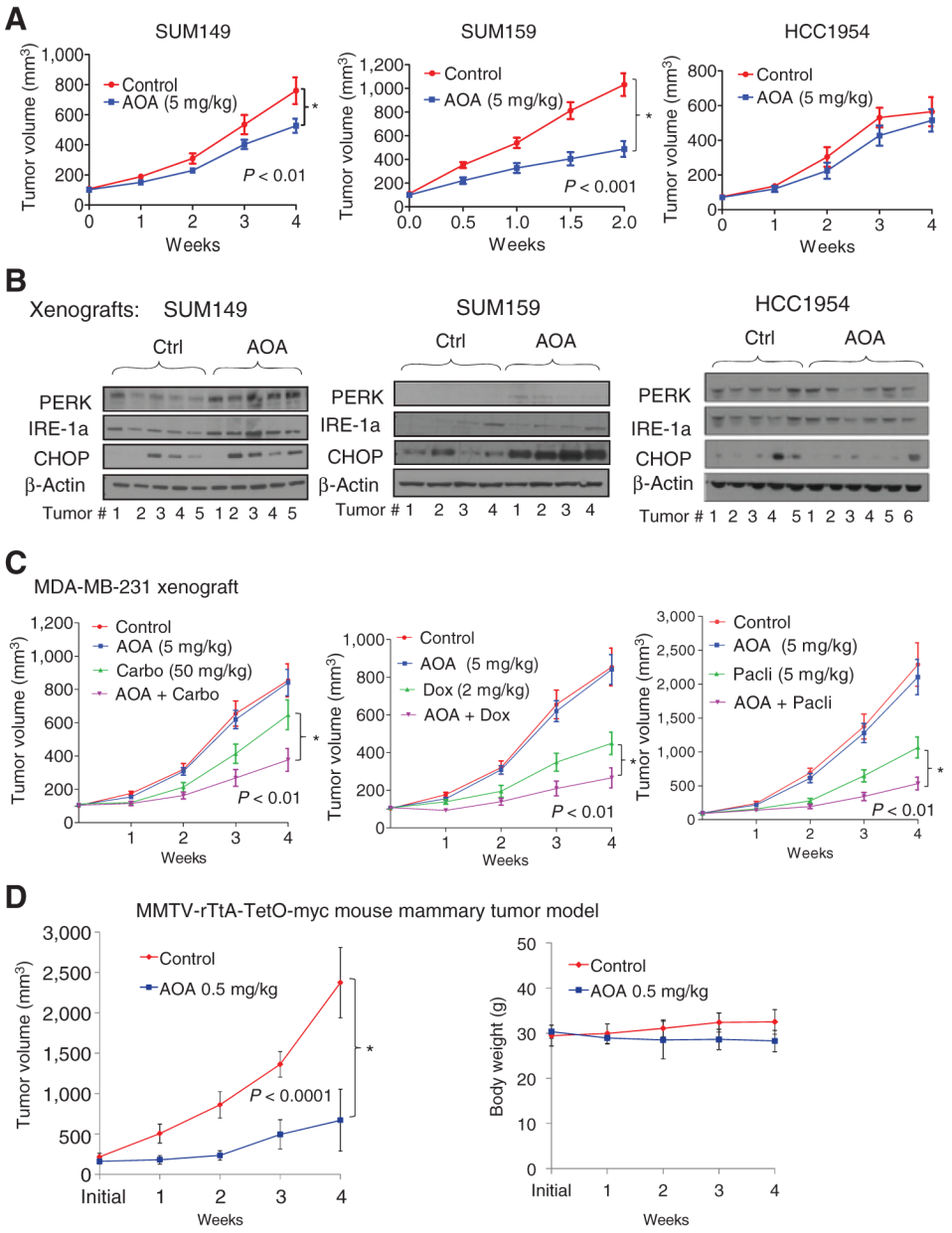

Figure 6.

In vivo growth inhibitory effect of AOA. A, SUM149, SUM159, or HCC1954 cells were injected s.c. into athymic Balb/c mice. When tumors reached a size of 100 mm^3, mice were randomized to control (PBS) or AOA (5 mg/kg i.p., daily) treatment (n = 6–8 mice/group). B, Western blot analysis of stress pathway markers in xenografts of SUM159, SUM149, and HCC1954. Tumors were collected at the end of experiment. C, In MDA-MB-231 xenografts, a combination of AOA with doxorubicin, carboplatin, or paclitaxel showed growth inhibitory effects. Data are plotted as the mean ± SEM and compared via mixed-effects models with the Tukey procedure for multiple testing corrections. D, left, tumor-bearing MMTV-rTtA-TetO-myc mice were treated with PBS (n = 10) or AOA 0.5 mg/kg (i.p. 3 days/week; n = 5). Treatment was initiated when the tumors reached 150 to 200 mm^3

and was continued for 4 weeks. Right, body weight of animals receiving AOA showed no significant decrease compared to vehicle-treated animals. ANOVA; *, $P = <0.0001$.